

# Analysis of Fracture Failure of Connecting Bolts for Diaphragm Pump Valve Box Cover

Xuan Qi, Yue Gao

Hainan University of Science and Technology, Haikou 571126, Hainan, China

**Copyright:** © 2026 Author(s). This is an open-access article distributed under the terms of the Creative Commons Attribution License (CC BY 4.0), permitting distribution and reproduction in any medium, provided the original work is cited.

**Abstract:** Aiming to address the repeated fracture of connecting bolts in the feed valve box cover of a large Type A diaphragm pump, a three-dimensional model of the valve box assembly was first established. Subsequently, bolt strength was evaluated using three finite element analysis methods: axisymmetric analysis, cyclic symmetry analysis, and full 3D integral analysis. It was clarified that the first few threads bear the maximum stress, which is consistent with the actual fracture position. Combined with the analysis results, it is concluded that the main causes of bolt fracture are alternating load bearing, low safety margin of specifications, and the coarse thread design also affects its load-bearing capacity.

**Keywords:** Diaphragm pump; Valve box cover bolt; Fracture analysis; Finite element analysis; Alternating load

**Online publication:** April 22, 2026

## 1. Introduction

The bolts of the inlet check valve cover (i.e., feed valve cover) of the large Type A diaphragm pump used by a pipeline company have fractured repeatedly, resulting in damage to the internal threads of the screw holes of the check valve chamber (i.e., valve box body). This has caused a great impact on the production of the pipeline company and brought huge potential safety hazards to its equipment. In response to this situation, the causes of bolt fracture and solutions are to be analyzed to restore the original design function of the equipment after repair.

## 2. Establishment of 3D model for valve box assembly parts

The maximum design pressure of the Type A diaphragm pump is 26 MPa, the outer ring diameter at the nominal diameter of the valve box port is 280 mm, the inner ring diameter is 251.2 mm, and the height between the inner and outer rings is 21 mm. Each valve box assembly is equipped with 4 M42 double-ended studs, the diameter at the middle necking part of the stud is 32.6 mm, and the total length of the stud is 265.5 mm<sup>[1]</sup>.

A 3D model of the valve box assembly was established according to the relevant drawings and partial actual dimensions provided by the company<sup>[2]</sup>. The outer ring diameter at the nominal diameter of the valve box port of the valve box 3D model is 270 mm, the inner ring diameter is 210 mm. According to the design pressure of

25 MPa, the bolt force on the connecting bolts between the valve box and the valve box cover is calculated as follows:

$$F = \frac{\pi}{4} \times 270^2 \times 25 \div 4 = 357665N$$

### 2.1. Establishment of 3D model for double-ended stud

The double-ended stud model was established in accordance with the GB/T899-1988 standard (Figure 1), with the main parameters as follows: nominal diameter:  $d = 42$  mm;  $Bm = 1.5$ ;  $d = 63$  mm;  $B = 96$  mm;  $l = 170$  mm; diameter at the middle necking part: 32.6 mm; total length of the stud: 233 mm [3].

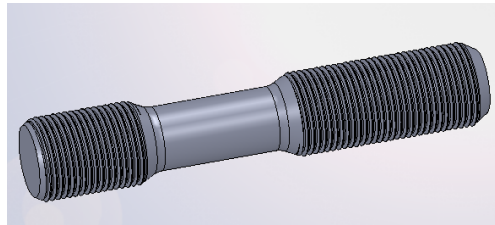


Figure 1. 3D model of double-ended stud.

### 2.2. Selection and establishment of thread profile

The connecting thread model was established in accordance with the GB/T196-1981 standard, with a pitch  $P = 3$  mm [4].

The profile and dimensions of the thread profile feature cutting are shown in Figure 2.

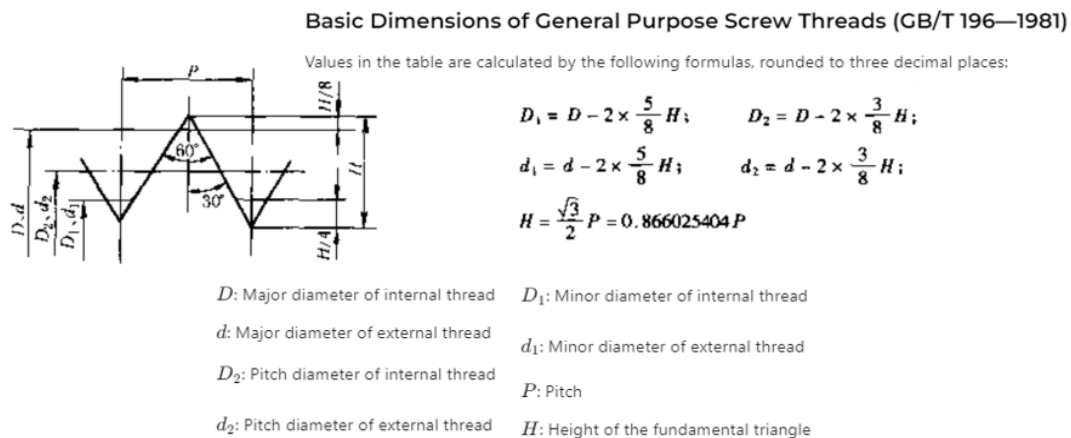
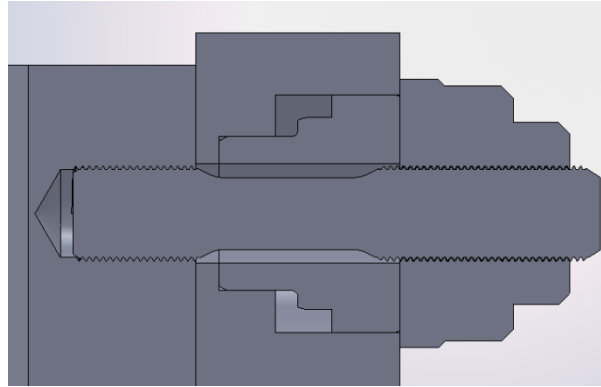


Figure 2. GB/T196-1981 general thread standard.

### 2.3. Assembly of feed valve box components

Considering that excessive thread contact will cause a serious decline in calculation speed, and most bolt fracture positions are at the end where the stud is screwed with the internal thread of the valve box, the two inner and outer nuts on the outer side of the valve cover were simplified into one nut, and the positions without actual dimensions of the valve box and valve cover were rounded [5]. The overall assembly of the feed valve box and the bolt connection section view of the established integral assembly model are shown in Figure 3.



**Figure 3.** Overall assembly of feed valve box and section view of bolt connection.

### 3. Finite element strength analysis methods for connecting bolts of feed valve box cover

The main work of finite element analysis for bolt connection problems lies in the mesh division at the thread profile and the establishment of contact pairs between internal and external threads. How to divide sufficiently fine meshes at the thread profile while avoiding an excessively large overall number of meshes under the condition of increased calculation time caused by contact pairs, thus ensuring good calculation speed and results, has become a key factor in bolt connection analysis [6].

In view of this, this paper adopts three methods: axisymmetric analysis, cyclic symmetric analysis and 3D analysis with bolt mesh division by a certain software, to calculate and analyze the simplified structure of bolt connection. That is, the model at the connection position between the double-ended stud and the valve box is extracted, the thread features at the connection between the double-ended stud and the nut are simplified, and the bolt force is used instead for analysis.

#### 3.1. Axisymmetric analysis method and results

The axisymmetric model was meshed with PLANE42 elements, the mesh size at the thread profile was set to 0.5 mm, and the overall mesh size was set to 2 mm, with a total of 3834 elements and 3926 nodes divided. The mesh and loading type are shown in **Figure 4**. Only the valve box model was fixed, and the outer side of the stud was subjected to bolt tension for analysis [7]. The nephogram of analysis results is as follows.

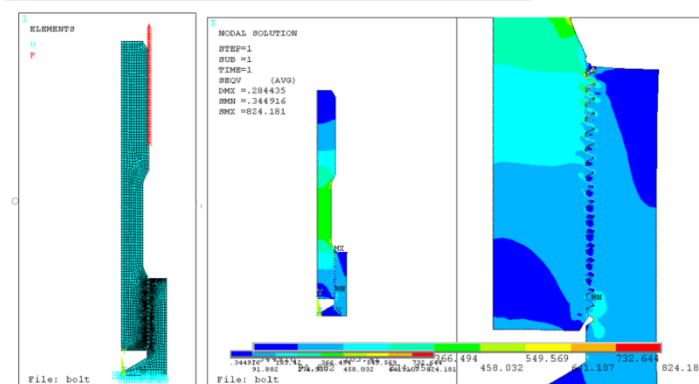


**Figure 4.** Mesh and load diagram of axisymmetric analysis for bolt connection, stress nephogram of axisymmetric analysis.

The maximum equivalent stress is  $\sigma = 824.181$  MPa, and the maximum deformation is  $\delta = 0.284$  mm. The maximum contact pressure on the double-ended stud reaches 364.65 MPa, while the stress at the necked middle section is 445.553 MPa. The maximum deformation at the threaded region is 0.058 mm.

Due to the pronounced non-uniform load distribution among threads, the first few threads typically carry a significantly higher load. Therefore, the stresses in the first seven threads were extracted and compared, as presented in **Table 1**.

**Table 1.** Stress comparison table of each thread circle in axisymmetric analysis

Thread position	1st circle	2nd circle	3rd circle	4th circle	5th circle	6th circle	7th circle
Equivalent stress (MPa)	824.181	566.552	451.625	398.963	380.250	357.260	300.901

### 3.2. Cyclic symmetric analysis method and results

The cyclic symmetric model was meshed with SOLID45 elements, the mesh size at the thread profile was 0.5 mm, and the overall mesh size was 2 mm, with a total of 16501 elements and 13001 nodes divided. The analysis working condition is the same as that of the axisymmetric analysis. The mesh and loading type are shown in **Figure 5**, and the nephogram of analysis results is as follows.

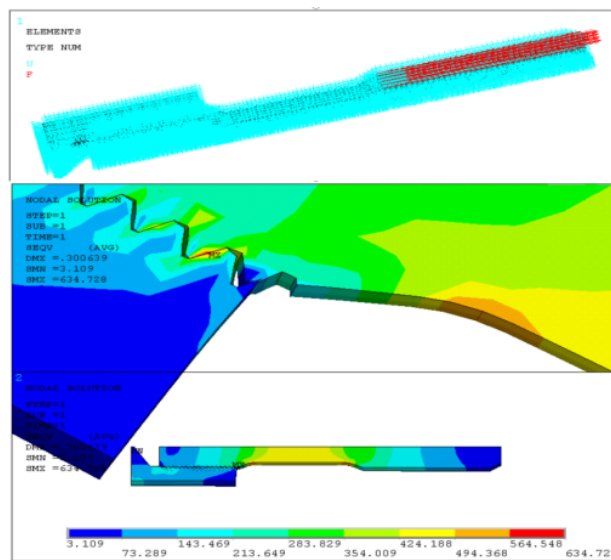


**Figure 5.** Load and constraint diagram of cyclic symmetric analysis for bolt connection, stress nephogram of cyclic symmetric analysis.

The maximum equivalent stress is  $\sigma = 634.728$  MPa, and the maximum deformation is  $\delta = 0.301$  mm. The maximum contact pressure on the double-ended stud is 284.936 MPa, while the stress at the necked middle section is 449.457 MPa. The maximum deformation in the threaded region is 0.061 mm.

The stress distribution in the first seven threads is presented in **Table 2**.

**Table 2.** Stress comparison table of each thread circle in cyclic symmetric analysis

Thread position	1st circle	2nd circle	3rd circle	4th circle	5th circle	6th circle	7th circle
Equivalent stress (MPa)	634.728	436.988	340.867	362.615	236.638	202.846	235.418

A curve graph of the stress at each thread circle from axisymmetric and cyclic symmetric analysis was drawn, as shown in **Figure 6**.

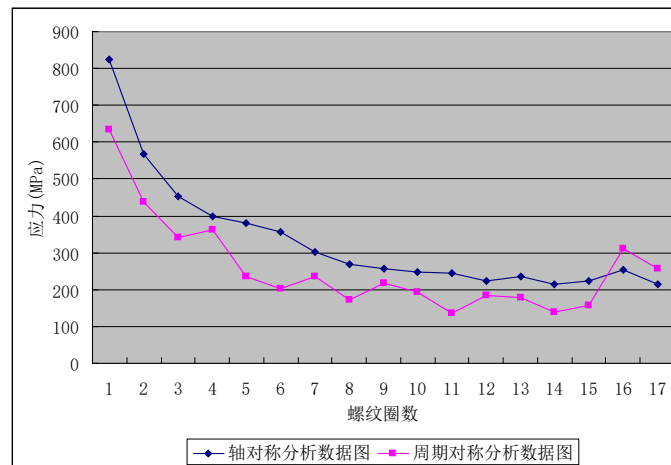


**Figure 6.** Stress comparison curve of each thread circle from axisymmetric and cyclic symmetric analysis.

It can be seen that the bolt stress change trends obtained by axisymmetric and cyclic symmetric analysis are basically the same. The curve smoothness of the axisymmetric analysis is better than that of the cyclic symmetric analysis, but the overall values are higher than those of the cyclic symmetric analysis. The reason may be that the axisymmetric model is meshed with tetrahedral elements, whose mesh quality is worse than that of the quadrilateral elements in the cyclic symmetric analysis, so the degree of element stress concentration may be slightly higher, resulting in higher values<sup>[8]</sup>.

Since the bolt stress is the largest at the thread circle with the maximum tension, which matches the nut thread circle with the maximum pressure, the uneven load distribution on the thread is increased. According to the force distribution diagram of each thread circle for the ten-thread nut proposed by N.E. Zhukovsky, the first thread circle bears the maximum load, accounting for about 1/3 of the total force on the screw, while the tenth thread circle at the end bears less than 1/100 of the total force. Due to the thread circle deformation caused by thread profile error, contact deformation and local plastic deformation, the load on the first thread circle is reduced to 1/5 or 1/4 of the total force.

It can be seen from **Figure 6** that the curve shape is basically in line with the law of N.E. Zhukovsky's thread load distribution diagram, and the curve formed by the axisymmetric analysis results is more continuous<sup>[9]</sup>.

### 3.3. Integral analysis method and results for bolt connection

The 3D integral model of bolt connection was taken, and meshed with SOLID45 elements by a certain analysis software, with the mesh size at the thread profile set to 0.5 mm and the overall mesh size set to 2 mm, with a total of 231508 elements and 54043 nodes divided. The analysis working condition is the same as that of the axisymmetric analysis. The load and constraint diagram is shown in **Figure 7**.

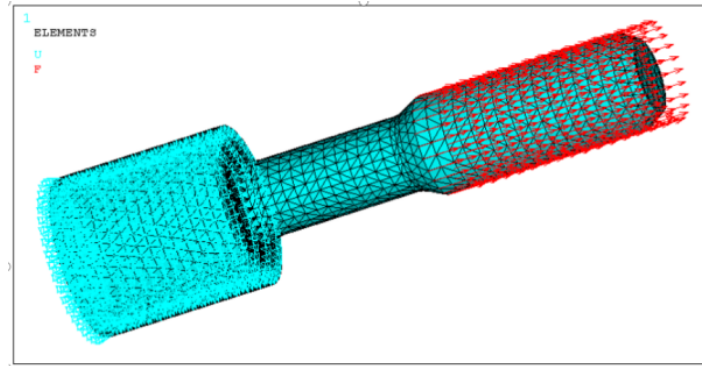


**Figure 7.** Load and constraint diagram of integral analysis for bolt connection.

After the 3D integral analysis of bolt connection, it was found that for different thread engagement positions, two different stress trends appeared: one is a nephogram with equidistant stress intensity law, and the other is a stress nephogram with normal distribution<sup>[10]</sup>. In response to this situation, different thread engagement angles were analyzed, and the basic law between the thread head-tail coincidence angle and the stress trend change was obtained. The detailed analysis content and results are shown in **Table 3**.

**Table 3.** Relationship between thread head-tail coincidence angle and stress trend change

Serial number	Coincidence angle (°)	External rotation angle (°)	Stress concentration strip area
1	90	0	6
2	60	30	0
3	30	60	6
4	0	90	0
5	270	180	6
6	180	270	0
7	45	45	6

The analysis results show that excluding the stress concentration points at the thread head-tail contact in bolt analysis, the maximum stress is between 800 and 1000 MPa, and the position is mostly at the first contact thread at the bolt root; the stress at the bolt head (far from the necking end) is large, and the stress at the middle part is small<sup>[11]</sup>.

In the 3D finite element analysis of bolt connection, stress concentration strip areas are likely to appear in the analysis results; there is no stress concentration strip area when rotating 30°, and the strip area appears again when rotating another 30°. In addition, the initial thread head-tail coincidence is 90°, and the area within 30° of the contact entry point is a low-stress area; this stress change law does not change with the change of bolt tension;

One side of the thread connection was set as a rigid body to observe the stress state of the other side. It was found that when the bolt external thread is rigid, the internal stress value of the valve box internal thread is the largest and gradually decreases outward; when the valve box internal thread is rigid, the stress value at the bolt external thread root is the largest and gradually decreases outward, and the maximum stress value reaches more than 1300 MPa<sup>[12]</sup>.

The mesh of the first few thread models with large stress was refined and submodel analysis was carried out,

and it was found that the stress increased slightly and the trend remained unchanged (**Figure 8**).

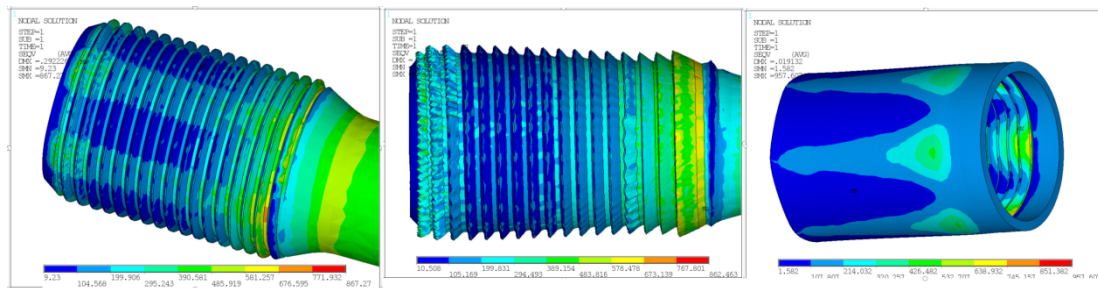


**Figure 8.** Stress nephogram with stress concentration strip area in bolt stress trend, stress nephogram without stress concentration strip area after adjusting thread head-tail coincidence angle, and bolt stress nephogram when internal and external threads are set as rigid bodies respectively.

#### 4. Overview of bolt fracture accident analysis

Due to the repeated fluctuation of the internal pressure of the feed valve box between the feed pressure and the discharge pressure, the connecting bolts of the feed valve box cover bear alternating loads, which causes more serious damage to the bolt material than the bolts of the discharge valve box cover, leading to bolt damage and even fatigue fracture<sup>[13]</sup>.

From the bolt strength analysis results, the first few threads usually bear relatively large stress, and the maximum stress is generally at the first complete thread circle, which is close to the actual fracture position of the bolt<sup>[14]</sup> (**Figure 9**).



**Figure 9.** Comparison diagram of bolt fracture positions.

The imported bolts used in on-site diaphragm pumps are generally coarse-pitch threads, and the proof load of fine-pitch threads with the same diameter is slightly higher than that of coarse-pitch threads<sup>[15]</sup>.

#### 5. Conclusion

According to the bolt specification selection calculation formula in domestic references, the specification of the connecting bolts for the feed valve box cover of the on-site diaphragm pump should be above M56. Compared with the strength analysis results of the diaphragm chamber cover bolts of the on-site diaphragm pump, it can be inferred that even if the bolt specification selection calculation formula of foreign standards is used to select the

feed valve box cover bolts, the safety margin of the bolts used for the feed valve box cover is still low.

## Disclosure statement

The authors declare no conflict of interest.

## References

- [1] Editorial Board of Mechanical Design Handbook, 2020, Mechanical Design Handbook: Volume 2 Fasteners, 6th Edition, China Machine Press, Beijing.
- [2] State Bureau of Technical Supervision, 1988, GB/T899-1988 Double-Ended Studs  $m=1.5d$ , China Standard Press, Beijing.
- [3] State Bureau of Technical Supervision, 1981, GB/T196-1981 Basic Dimensions of General Purpose Metric Screw Threads, China Standard Press, Beijing.
- [4] Wang X, Shao M, 2003, Basic Principles and Numerical Methods of Finite Element Method, 2nd Edition, Tsinghua University Press, Beijing.
- [5] Liu H, 2017, Mechanics of Materials (I), 6th Edition, Higher Education Press, Beijing.
- [6] Gou W, Jin B, Wei F, 2008, Mechanical Fatigue and Fracture, Northwestern Polytechnical University Press, Xi'an.
- [7] Zhang F, 2014, Design and Application of Threaded Connections, China Machine Press, Beijing.
- [8] Wang G, 2008, Practical Engineering Numerical Simulation Technology and Its Application in ANSYS, 2nd Edition, Northwestern Polytechnical University Press, Xi'an.
- [9] Editorial Board of Mechanical Engineering Materials Handbook, 2019, Mechanical Engineering Materials Handbook: Metal Materials Volume, 5th Edition, Chemical Industry Press, Beijing.
- [10] Zheng J, Dong Q, Sang Z, 2015, Process Equipment Design, 4th Edition, Chemical Industry Press, Beijing.
- [11] Yu W, Gao B, 2017, Application of ANSYS in Mechanical and Chemical Equipment, 3rd Edition, China Water & Power Press, Beijing.
- [12] He X, 2011, Mechanical Connection Technology, China Machine Press, Beijing.
- [13] National Technical Committee for Pump Standardization, 2021, JB/T6900-2021 Diaphragm Pumps, China Machine Press, Beijing.
- [14] Cheng D, 2017, Handbook of Taboos in Mechanical Design, 2nd Edition, Chemical Industry Press, Beijing.
- [15] Li H, 2011, Hydraulic Components and Systems, National Defense Industry Press, Beijing.

### Publisher's note

Bio-Byword Scientific Publishing remains neutral with regard to jurisdictional claims in published maps and institutional affiliations.